

NATURAL CORONAGRAPHIC OBSERVATIONS OF THE ECLIPSING T TAURI SYSTEM KH 15D: EVIDENCE OF ACCRETION AND BIPOLAR OUTFLOW IN A WEAK-LINE T TAURI STAR¹

CATRINA M. HAMILTON² AND WILLIAM HERBST

Department of Astronomy, Wesleyan University, Middletown, CT 06459; catrina@astro.wesleyan.edu, bill@astro.wesleyan.edu

REINHARD MUNDT AND CORYN A. L. BAILER-JONES

Max-Planck-Institut für Astronomie, Königstuhl 17, D-69117 Heidelberg, Germany; mundt@mpia-hd.mpg.de, calj@mpia-hd.mpg.de

AND

CHRISTOPHER M. JOHNS-KRULL

Department of Physics and Astronomy, Rice University, 6100 Main Street, Houston, TX 77005; cmj@rice.edu

Received 2003 April 17; accepted 2003 May 21; published 2003 June 6

ABSTRACT

We present high-resolution ($R \sim 44,000$) UV-Visual Echelle Spectrograph spectra of the eclipsing pre-main-sequence star KH 15D covering the wavelength range 4780–6810 Å obtained at three phases: out of eclipse, near minimum light, and during egress. The system evidently acts as a natural coronagraph, enhancing the contrast relative to the continuum of hydrogen and forbidden emission lines during eclipse. At maximum light, the $H\alpha$ equivalent width was ~ 2 Å and the profile showed broad wings and a deep central absorption. During egress, the equivalent width was much higher (~ 70 Å) and the broad wings, which extend to ± 300 km s⁻¹, were prominent. During eclipse totality, the equivalent width was less than during egress (~ 40 Å) and the high-velocity wings were much weaker. $H\beta$ showed a somewhat different behavior, revealing only the blueshifted portion of the high-velocity component during eclipse and egress. [O I] $\lambda\lambda 6300, 6363$ lines are easily seen both out of eclipse and when the photosphere is obscured and exhibit little or no flux variation with the eclipse phase. Our interpretation is that KH 15D, although clearly a weak-line T Tauri star by the usual criteria, is still accreting matter from a circumstellar disk and has a well-collimated bipolar jet. As the knife-edge of the occulting matter passes across the close stellar environment, it is evidently revealing structure in the magnetosphere of this pre-main-sequence star with unprecedented spatial resolution. We also show that there is only a small, perhaps marginally significant change in the velocity of the K7 star between the maximum light and egress phases probed here.

Subject headings: accretion, accretion disks — line: profiles — stars: individual (KH 15D)

1. INTRODUCTION

KH 15D is a unique system in which a pre-main-sequence star is periodically occulted by extended nonluminous matter, presumably part of a circumstellar disk (Herbst et al. 2002). Every 48.36 days, the star fades over 2–3 days by ~ 3.5 mag and remains near minimum light for ~ 20 days. The eclipse duration has been increasing with time, by ~ 1 –2 days yr⁻¹. Hamilton et al. (2001) obtained low-resolution spectra in and out of eclipse and concluded that the star was a K7 weak-line T Tauri star (WTTS). The WTTS classification, based on the equivalent width (EW) of the $H\alpha$ line out of eclipse, is supported by the lack of any IR³ or UV excess emission and the absence of substantial photometric variability outside of eclipse. On the basis of its membership in NGC 2264 (Sung, Bessel, & Lee 1997), the estimated mass of the K7 star is 0.5 – $1 M_{\odot}$ and its age is 2–4 Myr.

In an attempt to learn more about this unique system, we obtained high-resolution spectra during the eclipse of 2001 December. We hoped to determine whether KH 15D is a radial velocity variable, whether there was evidence for additional light in the system beyond that of the K7 star, and whether the occultation had any effect on the spectrum. In fact, we found dramatic changes in the line profiles of $H\alpha$ and $H\beta$, as well as weak forbidden emission lines that become much more vis-

ible during eclipse. Evidently, the KH 15D system behaves like a “natural coronagraph,” allowing us to see details of its close circumstellar environment during eclipse. Our evidence suggests that this WTTS is actively accreting gas and driving a bipolar outflow, although probably not at the rate of a typical classical T Tauri star (CTTS). This calls into question the common practice of associating WTTS characteristics with the absence of an accretion disk.

2. OBSERVATIONS AND THE ABSORPTION SPECTRUM

High-resolution echelle spectra of KH 15D were obtained on the nights of UT 2001 November 29, when it was in its bright state just prior to eclipse, on UT 2001 December 14, just past mideclipse, and again on UT 2001 December 20 during egress (see Fig. 1). These data were collected with the UV-Visual Echelle Spectrograph (UVES) on the European Southern Observatory’s Very Large Telescope (VLT), at Mount Paranal, Chile. The wavelength range is ~ 4780 – 6810 Å. A 50 Å gap centered on 5800 Å is present because of use of the red arm, which employs a mosaic of two 4096×2048 CCDs (D’Odorico et al. 2000). With a $1''$ slit, the spectral resolution is $\sim 44,000$. The spectra presented here were reduced via the UVES pipeline.⁴ As a check on this, the spectra were also reduced in the manner described by Valenti (1994). Both procedures make use of a sky subtraction algorithm. No significant differences were found between the data reduced by these techniques, and the UVES pipeline reduction is adopted here.

¹ Based on UV-Visual Echelle Spectrograph observations collected at the European Southern Observatory’s Very Large Telescope via Director’s Discretionary Time, within the observing program P267.C-5736.

² Department of Physics, Wesleyan University, Middletown, CT 06459.

³ $H-K = 0.14$, $K-L = 0.03$ out of eclipse; K. Haisch 2002, private communication.

⁴ Information regarding the reduction process can be found at <http://www.eso.org/instruments/uves>.

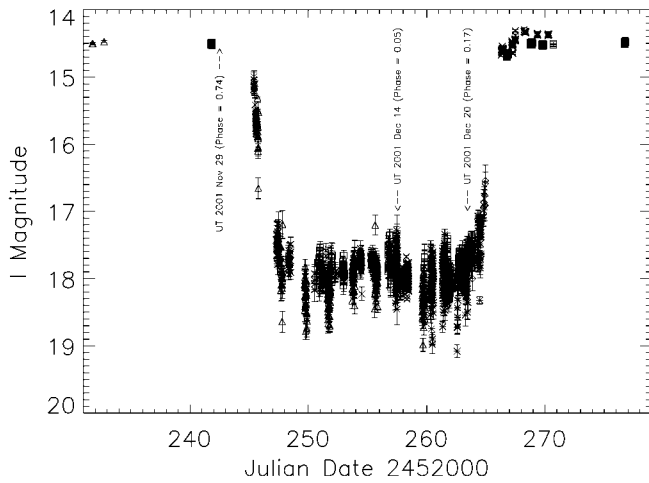


FIG. 1.—2001 December eclipse of KH 15D; photometry from Herbst et al. (2002). Arrows indicate epochs at which the UVES spectra were obtained.

The UVES spectra confirm that, out of eclipse, the primary light source in the KH 15D system is a K7 WTTS. The November 29 spectrum was visually compared in detail to 61 Cyg B, a typical K7 V, to look for any evidence of a second source of light in the system. No additional features were found. This spectrum was also compared to a rotationally broadened synthetic K7 V template to determine its $v \sin i$, which we estimate to be less than 5 km s^{-1} . The EW of the Li I 6707 feature is $0.401 \pm 0.001 \text{ \AA}$, consistent with the value of $0.47 \pm 0.05 \text{ \AA}$ measured on a low-resolution spectrum by Hamilton et al. (2001).

The out-of-eclipse spectrum was cross-correlated against HD 55999, a standard observed on the same nights, to determine the radial velocity of KH 15D. This was done with the IRAF⁵ task FXCOR. Since the spectra were obtained on two CCDs covering different wavelength regions, a cross-correlation was performed on each, avoiding the emission-line regions of H α and H β . A

⁵ Image Reduction and Analysis Facility, written and supported by the IRAF programming group at the National Optical Astronomy Observatory (NOAO) in Tucson, Arizona. NOAO is operated by the Association of Universities for Research in Astronomy, Inc., under cooperative agreement with the National Science Foundation.

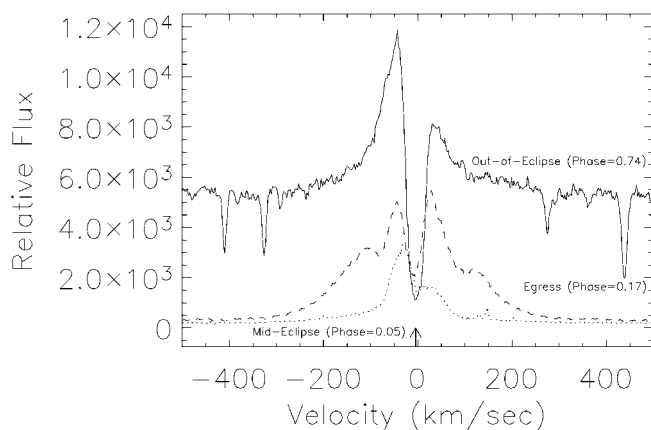


FIG. 2.—H α profiles of KH 15D obtained with the VLT and UVES during the 2001 December eclipse. The arrow indicates where the nebular emission of H α is seen in the background. The velocities are shown in the reference frame of the star.

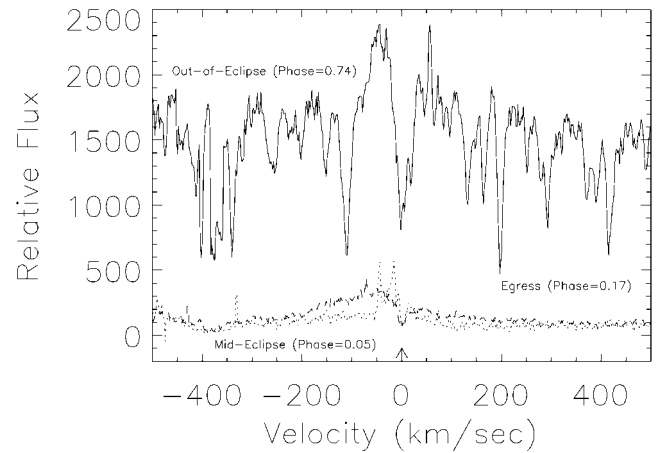


FIG. 3.—H β profiles of KH 15D obtained with the VLT and UVES during the 2001 December eclipse. The arrow indicates where the nebular emission of H β is seen in the background. The velocities are shown in the reference frame of the star.

heliocentric radial velocity of $+9.0 \pm 0.2 \text{ km s}^{-1}$ was found by this procedure for KH 15D on 2001 November 29.

The egress spectrum was cross-correlated against the out-of-eclipse spectrum in the same manner to look for any radial velocity variation between November 29 and December 20. A difference in heliocentric radial velocity of $3.3 \pm 0.6 \text{ km s}^{-1}$ was found. The radial velocity of the star on December 20 was, therefore, $+12.3 \pm 0.6 \text{ km s}^{-1}$. Whether this detection of radial velocity variation means that the K7 star is a spectroscopic binary remains to be seen. Photospheric line profile variations are expected in a partially eclipsed star, and the likely importance of scattered radiation near minimum light further complicates the interpretation. Clearly, a more extensive radial velocity study of the system is needed and is underway (J. Johnson & G. Marcy 2003, private communication).

3. THE EMISSION-LINE SPECTRUM

In Figures 2–4, we show the H α , H β , and [O I] $\lambda 6300$ emission-line profiles for KH 15D. Each spectrum has been flux calibrated to a relative scale using an R magnitude for the date, as given in Table 1. The quoted uncertainties on the magnitudes

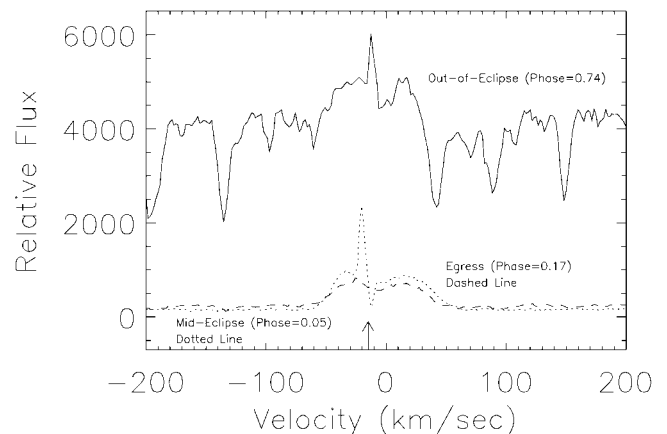


FIG. 4.—[O I] $\lambda 6300$ profiles of KH 15D obtained with the VLT and UVES during the 2001 December eclipse. The arrow indicates where the night-sky emission of [O I] has not been removed completely. The velocities are shown in the reference frame of the star.

TABLE 1
JOURNAL OF OBSERVATIONS AND MEASUREMENTS

JD (+2,452,000...)	V (mag)	R (mag)	I (mag)	EW _(Hα) (\AA)	EW _([O I]) (\AA)	Flux _(Hα) ^a ($\times 10^{-6}$)	Flux _([O I]) ^a ($\times 10^{-6}$)
242.7296	16.10 \pm 0.02	15.27 \pm 0.02	14.49 \pm 0.02	2.11 \pm 0.08	0.22 \pm 0.04	1.6 \pm 0.06	0.17 \pm 0.03
257.7840	19.6 \pm 0.1	18.9 \pm 0.1	18.2 \pm 0.1	39.3 \pm 1.5	8.4 ^b \pm 0.2	1.1 \pm 0.04	0.24 \pm 0.02
263.6871	19.1 \pm 0.1	18.3 \pm 0.1	17.6 \pm 0.1	70.8 \pm 5.1	3.1 \pm 0.2	3.4 \pm 0.24	0.15 \pm 0.02

^a Calculated as $\text{EW}_{(\text{H}\alpha)} \times 10^{-0.4R}$.

^b This EW was measured with the spike removed.

reflect a small degree of nonsimultaneity in the spectral and photometric data as well as the need to transform from I (where the data were more numerous) to R . Since spectral and photometric data were taken within an hour of each other, except at maximum light (when the brightness is nearly constant with time), and since the color variation is quite small (~ 0.1 mag in $R-I$ over the full brightness range), the uncertainty in R is only ~ 0.1 mag. Julian dates for each observation, measured I magnitudes, derived R and V magnitudes, measured EWs, and derived H α and [O I] fluxes are listed in Table 1. The EW measurements refer to the entire profile, both red- and blueshifted components combined. In Figures 2 and 3, the arrows indicate where H I nebular emission could have affected the profile, whereas in Figure 4 the arrow indicates where [O I] $\lambda 6300$ from the night sky may not have been removed completely.

Figure 2 shows that dramatic changes occurred in the H α emission-line profile of KH 15D during eclipse and egress. Out of eclipse, the star appears to be a WTTS with an $\text{EW}(\text{H}\alpha) \sim 2$ \AA but with a double-peaked profile, having a central absorption and faint but clearly detectable broad wings. A comparison with the H α profiles of other WTTSs (Hartmann 1982; Mundt et al. 1983; Finkenzeller & Basri 1987; Edwards et al. 1994; Reipurth, Pedrosa, & Lago 1996) shows that only three out of 19 such stars exhibited double-peaked profiles similar to KH 15D, with UX Tau A being the most similar (see Reipurth et al. 1996). Most WTTSs show narrow single-peaked emission lines. It is also interesting that the central absorption feature appears to extend below the stellar continuum. This is unusual for any TTS, weak or classical. During eclipse and egress, the natural coronagraph effect is clear. Near mideclipse, the EW of H α grows to ~ 40 \AA , while the relative flux drops by $\sim 50\%$. During egress, the EW rises to ~ 70 \AA , as the flux increases, exceeding even its out-of-eclipse value. In all cases, a double-peaked profile is observed. The emission-line profile during mideclipse extends to ± 200 km s^{-1} with significantly less flux in the extended wings, as compared to the profile during egress, which extends to ± 300 km s^{-1} .

Figure 3 shows the corresponding H β line profiles. Again, dramatic EW and line profile changes are evident. Although the out-of-eclipse H β line profile is heavily affected by the underlying stellar absorption spectrum, it is similar to H α . In the egress spectrum, however, the emission occurs primarily on the blue side with a wing extending to -300 km s^{-1} . The asymmetry in this line is much more striking than H α . During mideclipse, although little H β flux is present, the shape of the line profile appears similar to egress. The weak features visible in this profile at -25 km s^{-1} are probably due to an improper background subtraction of the H β emission from NGC 2264.

Figure 4 shows the emission-line profiles for the [O I] $\lambda 6300$ line. The [O I] line, which is weak but clearly discernable at maximum light, becomes prominent at mideclipse and during egress. The line flux seems to be about the same out of eclipse and during egress, although slightly higher at mideclipse. We cau-

tion against any extreme interpretation of this measurement. The profile during mideclipse was disturbed by an improper background subtraction, and we feel that our errors are most likely underestimated. However, this behavior would indicate that none of the [O I]-emitting zone suffers variable occultation at the phases of our observations. This is fully expected, given the spatial extent of the (bipolar) forbidden line-emitting regions in CTTSs. The peak of the high-velocity component of the [O I] emission in typical CTTSs originates at about 30 AU from the star (Hirth, Mundt, & Solf 1997).

The EW of the [O I] $\lambda 6300$ line in the out-of-eclipse spectrum is about 0.17 \AA , which is quite large for a WTTS. Only one of the 10 WTTSs in Table 3 of Hartigan, Edwards, & Ghandour (1995) has a detectable [O I] $\lambda 6300$ line (with an $\text{EW} = 0.5$ \AA). The others have upper limits of about 0.06 \AA . Most CTTSs in that table, on the other hand, have EWs of 0.5–3 \AA . The profiles obtained during mideclipse and egress suggest that we have two emission peaks, at about -20 and $+18$ km s^{-1} with emission wings extending -60 to $+50$ km s^{-1} , respectively. These profiles are quite different from the [O I] $\lambda 6300$ profile seen in most strong emission CTTSs (with strong veiling), which often have a high-velocity component at -100 to -150 km s^{-1} (resulting from the jet) and a low-velocity component at about -20 km s^{-1} (Hartigan et al. 1995; Hirth et al. 1997). In addition, the profile is quite different from that of a CTTS with small veiling and IR excess (see the bottom profile in Fig. 11 of Hartigan et al. 1995). These latter profiles are usually single-peaked and unshifted in velocity. Although the profile shape for KH 15D is not fully clear because of imperfect subtraction of the emission of [O I] at 6300 \AA in the night sky, it is most likely double-peaked. Such a profile can be most easily explained by a bipolar jet moving nearly perpendicular to the line of sight, quite consistent with our expectation that the disk associated with KH 15D is viewed nearly edge-on, resulting in a very small radial velocity separation between the two jets. The profile catalog of Hartigan et al. (1995) contains several examples of bipolar jet sources (RW Aur, AS 353A, DD Tau), where the two jet components are clearly separated because of favorable inclination angles.

4. DISCUSSION

It is important to keep in mind that we do not yet know the geometry of the KH 15D system. In particular, it is not certain whether the occultation proceeds along a line perpendicular to or parallel to the rotation axis of the K7 star (or neither) or to what extent the rotation axis, the presumed stellar magnetic axis, and the orbital plane are aligned. It is not even known whether, relative to the system's center of mass, it is the K7 star or the occulting matter that is primarily in motion. Detailed modeling of the system must obviously await clarification of these basic issues. However, a preliminary qualitative interpretation of the emission-line variations is possible and provided in this section.

We believe that the observed spectral variations of KH 15D can be understood qualitatively in terms of a weakly accreting “scaled down” CTTS (see, e.g., Muzerolle, Calvet, & Hartmann 2001), whose photosphere and magnetosphere are periodically occulted by a relatively sharp knife-edge (as described in Herbst et al. 2002, their Fig. 5). We expect such a star to have a bipolar jet region, which we assume, by analogy with the CTTS, is revealed by the forbidden emission-line radiation. Assuming a jet velocity of 200 km s^{-1} (which is the average jet velocity for CTTSs derived by Hirth et al. 1994) and adopting a radial velocity of $\pm 20 \text{ km s}^{-1}$ for the [O I] $\lambda 6300$ peaks, we derive an inclination angle for the jet to the line of sight of 84° . This is consistent with a general picture for the system in which we view the K7 star close to the orbital plane of its circumstellar (or circumbinary) disk and the jets emerge roughly perpendicular to the disk plane, as for the star associated with HH 30 and other examples imaged by the *Hubble Space Telescope* (Ray et al. 1996). The absence of any significant variation in the profiles or flux of the forbidden line radiation during eclipse is consistent with the expectation, based on the CTTS analogy, that it arises at distances of tens of AUs from the star, beyond the region variably occulted.

The behavior of the hydrogen lines is complex, because some components do arise close to the star and, therefore, suffer variable occultation effects along with the photosphere. Since we expect that the $H\alpha$ line has a much higher optical depth than the $H\beta$ line, it is obvious that any emission-line region will be more extended in $H\alpha$ than $H\beta$. If we assume that the magnetic axis of the K7 star is tilted toward us at $\sim 5^\circ$ – 10° , which is a reasonable assumption supported by the [O I] line profiles, at mideclipse, one can qualitatively understand the $H\alpha$ line profile as resulting from low-velocity material in the outer, more extended $H\alpha$ emission region while the star and the $H\beta$ line-forming region are obscured by the occulting disk material. This would also explain why there is almost no $H\beta$ flux during mideclipse. During egress, we expect most of the $H\alpha$ emission-line region, as well as some of the $H\beta$ emission-line region, which is closer to the star, to be visible. The $H\alpha$ line profile during egress has a low-velocity emission peak with a central absorption feature similar to what is seen in the out-of-eclipse profile. Additionally, two “shoulders” appear along the profile at about $\pm 150 \text{ km s}^{-1}$ extending out to $\pm 300 \text{ km s}^{-1}$. These shoulders could be due to material rotating in the outer parts of the magnetosphere. However, given that the $v \sin i$ is measured to be less than 5 km s^{-1} and that the magnetosphere extends out to only about 5–6 stellar radii, the maximum rotational velocity is about 5–6 $v \sin i$ or 25–30 km s^{-1} , making

it difficult to explain the $H\alpha$ emission-line profile with a rotating magnetosphere.

A more attractive hypothesis is that the high-velocity shoulders on the $H\alpha$ line, so prominent in the egress spectrum, arise from material falling along magnetic accretion columns. This interpretation can also qualitatively account for the $H\beta$ emission-line profile during egress. Adopting values for the mass and radius of the K7 star from Table 1 of Hamilton et al. (2001), a free-fall velocity of about 380 km s^{-1} can be associated with material at the surface of the star. Since $H\beta$ is produced much closer to the star, the blueshifted wing extending to nearly -350 km s^{-1} could be representative of material accreting along magnetic field lines near the pole. The asymmetry seen in the $H\beta$ emission-line profile is most likely due to the fact that the star is slightly inclined toward our line of sight. The reappearance of both a blue and a red wing to the $H\alpha$ line during the early part of egress, when most of the stellar photosphere is still occulted, shows that both redshifted and blueshifted gas is present along the same line of sight toward the small portion of the photosphere and magnetosphere that is being uncovered first. This also supports an accretion interpretation as opposed to, say, a rotation interpretation for the high velocities.

5. CONCLUSIONS

It appears that KH 15D, although clearly a WTTS by the usual criteria of weak $H\alpha$ emission, absence of UV or IR excess emission, and relative photometric stability, is still undergoing active accretion and driving a bipolar outflow. It provides a cautionary example against assuming that all stars with WTTS characteristics no longer have accretion disks. The unique geometry of this system, in which a relatively sharp-edged occulting mask crosses the photosphere, has created a natural coronagraph that enhances the visibility of the star’s magnetosphere during eclipse. The occultation also evidently crosses the inner portion of the star’s magnetosphere, where high-velocity gas motions arise, probably from magnetically channeled accretion. Synoptic studies of this star ultimately may allow us to reconstruct aspects of the structure of its magnetosphere with spatial resolution that will be unobtainable in other objects for decades to come.

We thank U. Bastian, M. Ibraghimov, J. Johnson, G. Marcy, F. Vrba, and J. Aufdenberg for helpful conversations and useful data on this star. W. H. acknowledges support from NASA through its Origins of Solar Systems program.

REFERENCES

- D’Odorico, S., et al. 2000, Proc. SPIE, 4005, 121
 Edwards, S., Hartigan, P., Ghandour, L., & Andriulis, C. 1994, AJ, 108, 1056
 Finkenzeller, U., & Basri, G. 1987, ApJ, 318, 823
 Hamilton, C. M., Herbst, W., Ferro, A. J., & Shih, C. 2001, ApJ, 554, L201
 Hartigan, P., Edwards, S., & Ghandour, L. 1995, ApJ, 452, 736
 Hartmann, L. 1982, ApJS, 48, 109
 Herbst, W., et al. 2002, PASP, 114, 1167
 Hirth, G. A., Mundt, R., & Solf, J. 1997, A&AS, 126, 437
 Hirth, G. A., Mundt, R., Solf, J., & Ray, T. P. 1994, ApJ, 427, L99
 Mundt, R., Walter, F. M., Feigelson, E. D., Finkenzeller, U., Herbig, G. H., & Odell, A. P. 1983, ApJ, 269, 229
 Muzerolle, J., Calvet, N., & Hartmann, L. 2001, ApJ, 550, 944
 Ray, T. P., Mundt, R., Dyson, J. E., Falle, S. A. E. G., & Raga, A. C. 1996, ApJ, 468, L103
 Reipurth, B., Pedrosa, A., & Lago, M. T. V. T. 1996, A&AS, 120, 229
 Sung, H., Bessel, M. S., & Lee, S. 1997, AJ, 114, 2644
 Valenti, J. 1994, Ph.D. thesis, Univ. California, Berkeley